

Observation of a Ternary Nanocrystal Superlattice and Its Structural Characterization by Electron Tomography**

Wiel H. Evers, Heiner Friedrich, Laura Filion, Marjolein Dijkstra, and Daniel Vanmaekelbergh*

The crystallization of nanometer-sized colloids and the three-dimensional structural characterization of the ensuing lattices is a relatively new field compared to that of the micrometer-sized colloids being studied extensively for decades. In the mid 1990s, it was shown that colloidal CdSe nanocrystals, the workhorse of colloidal quantum dots, form a superlattice upon drying of the suspension.^[1] Several years later, again in analogy with micrometer-sized colloids, it was reported that gold nanocrystals of two different diameters form binary superlattices.^[2] Since then, a plethora of different binary superlattices composed of metallic, magnetic, and semiconductor nanocrystals have been demonstrated.^[3–9] The research has been driven mostly by the aim of forming novel metamaterials, with collective properties that result from interactions between nanometer-sized semiconductors, metals, and magnets in close contact in a well-ordered 3D geometry. Many of the known atomic binary lattices now have their counterparts in crystals of both micrometer-^[10] and nanometer-sized colloids.

Atomic lattices can also consist of three or more different types of atoms. However, the colloidal counterpart of a ternary atomic lattice has not been observed to date. Herein, we report a genuine ternary nanocrystal (NC) superlattice ABC_4 composed of three different nanocrystals; that is, A = PbSe NCs of (12.1 ± 0.4) nm diameter, B = PbSe NCs of (7.9 ± 0.3) nm, C = CdSe NCs of (5.8 ± 0.3) nm.^[11] We studied colloidal crystallization upon evaporation of the solvent from a suspension that contains these nanocrystals in relative concentration ratios $[B]/[A] = 1.3$, $[C]/[A] = 10.9$. We observe ternary domains ABC_4 , isostructural with the atomic lattice $AlMgB_4$, formed together with the binary superlattices AC_2 (isostructural with AlB_2) and BC_2 (isostructural with $MgZn_2$).

The 3D structure of this genuine ternary nanocrystal superlattice has been studied in detail with electron tomography.

Upon evaporation of the solvent from the ternary suspension, nanocrystal films are formed on the TEM grid. Some regions on the TEM grid display ordered domains (superlattices) with lateral dimensions in the $1 \mu\text{m}$ range. Besides a small percentage of single-component superlattices, three different crystal structures could be distinguished: domains of binary AC_2 and BC_2 superlattices, together with domains of a ternary superlattice that contains the large and medium-sized PbSe NCs and the CdSe NCs. Figure 1 shows a TEM projection of the ternary superlattice; the three different nanocrystals are clearly visible in the TEM projection (see also the overlay). We observed that the ternary domains are epitaxially connected to binary AC_2 domains (the dashed line in Figure 1 depicts such an epitaxial interface). The binary lattice on the top right corner of Figure 1 is isostructural with AlB_2 . The ternary lattice can be derived from the binary lattice by substituting every second vertical layer of large PbSe NCs (blue in the overlay) by medium-sized PbSe NCs (green in the overlay). In fact, Figure 1 shows the (100) plane of the ternary ABC_4 structure, which was identified as isostructural with the atomic $AlMgB_4$ crystal. The ternary

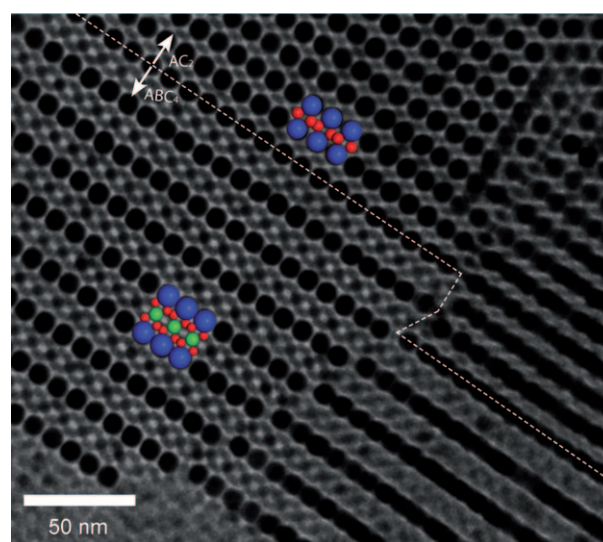


Figure 1. TEM projection of the ternary ABC_4 , that is, $[PbSe(l)]-[PbSe(m)][CdSe(s)]_4$ nanocrystal superlattice (l = large, m = medium, s = small) in epitaxial contact with the binary AC_2 superlattice $[PbSe(l)]-[CdSe(s)]_2$. The TEM picture and cartoon show the (100) plane of the ternary superlattice, in which the large PbSe NCs (blue spheres), medium-sized PbSe (green spheres), and small CdSe (red spheres) can be observed individually. The ternary nanocrystal superlattice is isostructural with $AlMgB_4$.

[*] W. H. Evers, Prof. D. Vanmaekelbergh
Condensed Matter and Interfaces
Debye Institute for NanoMaterials Science, University Utrecht
Princetonplein 1, 3584 CC, Utrecht (The Netherlands)
Fax: (+31) 30-253-2403
E-mail: d.vanmaekelbergh@uu.nl

Dr. H. Friedrich
Inorganic Chemistry and Catalysis
Debye Institute for NanoMaterials Science, University Utrecht
Sorbonnelaan 16, 3584 CA, Utrecht (The Netherlands)

L. Filion, Prof. M. Dijkstra
Soft Condensed Matter
Debye Institute for NanoMaterials Science, University Utrecht
Princetonplein 1, 3584 CC, Utrecht (The Netherlands)

[**] W.H.E. acknowledges NWO-CW (grant 700.53.308) for financial support.

Supporting information for this article is available on the WWW under <http://dx.doi.org/10.1002/anie.200904821>.

domains that we have analyzed always have the (100) plane parallel to the substrate surface. A 3D model of this crystal as observed herein (substrate on the bottom) is presented in Figure 2e. We note that in the ordered regions of the TEM grid BC₂ binary superlattices (consisting of medium-sized PbSe NCs and small CdSe NCs) are also observed, which are isostructural with MgZn₂.

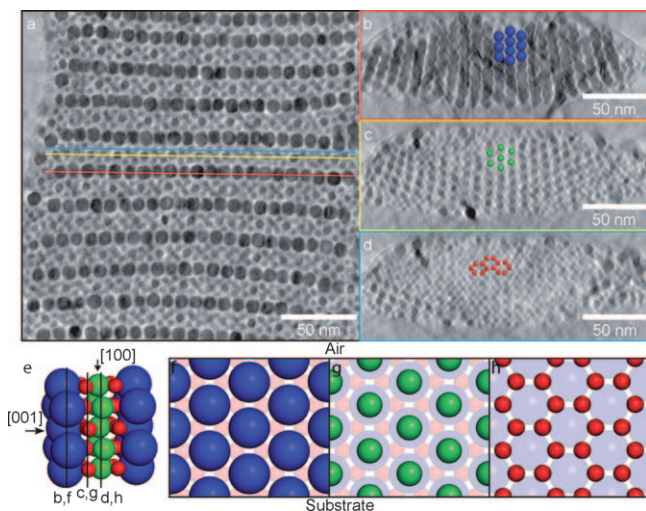


Figure 2. Tomographic analysis of the ternary ABC₄ structure. a) A horizontal cross section through the center of the large PbSe NCs lying in the [100] plane of the 3D reconstructed lattice. The cross section also cuts through half of the medium-sized PbSe and small CdSe nanocrystals. The colored lines show the positions of the vertical cross sections through the center of the large PbSe NCs (red), medium-sized PbSe NCs (yellow) and small CdSe NCs (blue) displayed in (b), (c), and (d), respectively. e) A model of the ternary structure as observed with the substrate on the bottom side. f–h) Models of the vertical cross sections through the large PbSe (blue), medium-sized PbSe (green), and small CdSe NCs (red), corresponding to the experimental cross sections in (b–d).

We performed electron tomography of the ternary domains by acquiring TEM projections over an angular range of 140° at 2° increments, with subsequent alignment of the data set by fiducial markers and reconstruction of the 3D lattice by weighted backprojection.^[8] Figure 2 shows numerical cross sections through a reconstructed ternary lattice; Figure 2a shows a horizontal cross section taken through the center of the larger PbSe nanocrystals of the ternary structure that has the [100] planes parallel to the substrate (see Figure 2e). The cross section also cuts through the center of half of the medium-sized PbSe and small CdSe NCs. It can be seen that the cores of the larger PbSe NCs are separated by the organic capping ligands. The colored lines indicate the positions of vertical cross sections displayed in Figure 2b–d. Figure 2b presents the vertical cross section through the center of the large nanocrystals. Strikingly, the PbSe cores seem to touch each other in the vertical direction; hence at these specific positions the organic capping ligands have disappeared. Note the difference with a cross section through the model lattice displayed in Figure 2f. The center-to-center distance in the vertical direction is about 8.0 nm on average,

which is equal to the core diameter. This lattice contraction is similar to what is observed with AlB₂ binary superlattices of PbSe and CdSe;^[8] we attribute this phenomenon to drying effects. Very probably, drying effects also cause the bending deformation of the ternary lattice visible in Figure 2b,c. Figure 2c presents a vertical cross section through the center of the medium-sized PbSe NCs. Note that the center-to-center distance is identical to that in the planes of the large PbSe nanocrystals. In fact, the medium-sized PbSe nanocrystals are positioned on the same sites as their larger counterparts (see also the model cross sections in Figure 2f,g). Figure 2d shows a vertical numerical cross section through the center of the small CdSe (model displayed in Figure 2f); the fact that at the boundaries large and medium-sized nanocrystals are also displayed is due to a slight bending of the overall lattice. We note that the AlMgB₄ structure that we observe is very similar to the AlB₂ binary structure. Hence, epitaxial boundaries between the ternary and binary lattices are no surprise (see the Supporting Information, Figure S1).

Finally, we discuss the possible reasons that genuine ternary structures are formed spontaneously in this system. At present, the driving force for the formation of binary nanocrystal superlattices is under discussion;^[6] some authors explain the stability of these crystal structures by entropy alone using packing arguments (for a basic discussion, see Ref. [12]); others speculate that the structures are stabilized by the interactions between the nanocrystals. Herein, we limit the discussion to the entropic contribution to the free energy of formation of the binary AlB₂^[13,14] and MgZn₂^[15] and ternary AlMgB₄ NC superlattices. The reason is that we have performed the colloidal crystallization at a relative high temperature (70°C), at which the entropy contribution to the free energy might possibly prevail.

Since we have three different sizes in the mixed suspension, we have to consider three size ratios: γ_1 = diameter CdSe NCs/diameter large PbSe NCs = 0.48, γ_2 = diameter CdSe NCs/diameter medium-sized PbSe NCs = 0.73, and γ_3 = diameter PbSe medium-sized/diameter large PbSe NCs = 0.65. For a size ratio of 0.48, the phase diagram of a binary mixture of hard spheres displays a stable binary superlattice AC₂, that is, PbSe(large NCs)/[CdSe NCs]₂, isostructural with AlB₂.^[13,14] Furthermore, recently calculated phase diagrams for binary hard-sphere mixtures using computer simulations show that the MgZn₂ lattice is stable for a size ratio between 0.76 and 0.84,^[15] hence just above γ_2 . In agreement with this finding, we observed that the ordered regions on the TEM grid are dominated by AlB₂-type AC₂ structures (about 65 % of the film) and MgZn₂-type BC₂ superlattices (about 25 % of the ordered film). To our knowledge there are no studies to date examining the stability of the ternary structure that we observe (occupying about 5 % of the ordered regions). Thus, to better understand the ternary structure we have calculated the maximum packing fraction of the AlMgB₄ lattice as a function of the size ratios γ_1 , γ_2 , and γ_3 (see the Supporting Information, Figure S2). From Figure S2 it can be shown that there is a region in γ_1 , γ_2 , γ_3 parameter space in which the ternary structure has a maximum packing fraction larger than that of the phase-separated mixture of AlB₂-type AC₂ with face-centered cubic crystals of the small and medium-sized

particles, thus demonstrating that in this region the ternary structure is stable at infinite pressure. At the experimental size ratios this criterion is not met, and thus the ternary crystal structure is not stable at infinite pressure.

While the maximum packing fraction of the ternary phase in the experimental system is quite low (ca. 0.64), this factor alone cannot be used to determine the stability of entropy-driven crystal structures at finite pressure. For instance, in a binary hard-sphere mixture of size ratio 0.76, the MgZn_2 phase has been theoretically found to be stable although its maximum packing fraction is only 0.67, similar to that of the ternary phase.^[15,16] Thus, full free energy calculations are needed to determine the stability of the ternary structure and to determine whether it can be stabilized at these size ratios by entropy alone, or whether cohesive forces are important.

In summary, we have presented the first genuine ternary colloidal crystal, which is a ternary superlattice composed of PbSe nanocrystals of two different diameters and of CdSe nanocrystals. TEM and electron tomography show that its structure is isostructural with the AlMgB_4 atomic lattice.

Experimental Section

PbSe nanocrystals were synthesized by a method described by Houtepen et al.^[17] The synthesis was performed in a water- and oxygen-free environment. 1) Lead acetate trihydrate (1.9 g, 99.999%, Aldrich), diphenyl ether (DPE, 4 mL, 99%, Aldrich), oleic acid (OA, 3 mL, 90%, Aldrich), and trioctylphosphine (TOP, 16 mL, 90%, Fluka) were heated to 100°C under low pressure (10–3 bar) for approximately 3 h. 2) A second mixture containing selenium (0.31 g, 99.999%, Alfa Aesar) and TOP (4 mL) was prepared. Subsequently, solution (1) (11.5 mL) and solution (2) (1.7 mL) were injected into DPE (10 mL) at 190°C. The reaction mixture was kept at a constant temperature of 145°C. After 30 seconds to 10 min, the reaction mixture was quenched with butanol (20 mL) and methanol (10 mL). The crude synthesis mixtures were washed twice by precipitating with methanol, centrifugation, and redispersion of the sediment in toluene.

CdSe nanocrystals were synthesized by a method described by de Mello Donegá et al.^[18] The synthesis was performed in a water- and oxygen-free environment. Selenium (0.79 g, 99.999%, Alfa Aesar), dimethylcadmium (0.28 g, 99.99%, ARC Technologies), and TOP (10 mL, 96%, Aldrich) were mixed. The solution was injected into a mixture of dried trioctylphosphine oxide (TOPO, 20 g, 99% Aldrich) and hexadecylamine (HAD, 10 g) at a temperature of approximately 300°C, resulting in a temperature drop to about 170°C. The temperature was raised and stabilized to the desired growth temperature of 240°C for 30 min, resulting in nanocrystals with a diameter of approximately 3 nm. The synthesis mixtures were washed twice by precipitating with methanol, centrifugation, and redispersion of the sediment in toluene.

Superlattice formation was achieved by mixing the three colloidal suspensions to obtain a mixed suspension containing the PbSe nanocrystals (A and B) and the CdSe NCs (C); the concentration ratio in this mixed suspension is approximately $[B]/[A] = 1.3$, $[C]/[A] = 10.9$, and $[C]/[B] = 8.2$. Colloidal crystallization was achieved on a TEM grid that makes an angle of 30° with the suspension surface, evaporating the solvent at a temperature of 70°C under reduced pressure.

Received: August 28, 2009

Published online: November 12, 2009

Keywords: nanoparticles · quantum dots · self-assembly · superlattices · ternary systems

- [1] C. B. Murray, C. R. Kagan, M. G. Bawendi, *Science* **1995**, 270, 1335.
- [2] C. J. Kiely, J. Fink, M. Brust, D. Bethell, D. J. Schiffrin, *Nature* **1998**, 396, 444.
- [3] F. X. Redl, K.-S. Cho, C. B. Murray, S. O'Brien, *Nature* **2003**, 423, 968.
- [4] E. V. Shevchenko, D. V. Talapin, N. A. Kotov, S. O'Brien, C. B. Murray, *Nature* **2006**, 439, 55.
- [5] Z. Y. Chen, J. Moore, G. Radtke, H. Sirringhaus, S. O'Brien, *J. Am. Chem. Soc.* **2007**, 129, 15702.
- [6] Z. Chen, S. O'Brien, *ACS Nano* **2008**, 2, 1219.
- [7] K. Overgaag, W. Evers, B. de Nijs, R. Koole, J. Meeldijk, D. Vanmaekelbergh, *J. Am. Chem. Soc.* **2008**, 130, 7833.
- [8] H. Friedrich, C. J. Gommers, K. Overgaag, J. D. Meeldyk, W. H. Evers, B. de Nys, M. P. Boneschanscher, P. E. de Jongh, A. J. Verkley, K. P. de Jong, D. Vanmaekelbergh, *Nano Lett.* **2009**, 9, 2719.
- [9] A. L. Rogach, *Angew. Chem.* **2004**, 116, 150; *Angew. Chem. Int. Ed.* **2004**, 43, 148.
- [10] M. E. Leunissen, C. G. Christova, A. P. Hynninen, C. P. Royall, A. I. Campbell, A. Imhof, M. Dijkstra, R. van Roij, A. van Blaaderen, *Nature* **2005**, 437, 235.
- [11] The diameters quoted here are derived from the center-to-center distances measured from TEM graphs of the single-component lattices of A, B, and C, respectively.
- [12] M. D. Eldridge, P. A. Madden, D. Frenkel, *Nature* **1993**, 365, 35.
- [13] M. D. Eldridge, P. A. Madden, P. H. Pusey, P. Bartlett, *Mol. Phys.* **1995**, 84, 395.
- [14] E. Trizac, M. D. Eldridge, P. A. Madden, *Mol. Phys.* **1997**, 90, 675.
- [15] A. P. Hynninen, L. C. Filion, M. Dijkstra, *J. Chem. Phys.* **2009**, 131, 064902.
- [16] L. Filion, M. Dijkstra, *Phys. Rev. E* **2009**, 79, 046714.
- [17] A. J. Houtepen, R. Koole, D. Vanmaekelbergh, J. Meeldijk, S. G. Hickey, *J. Am. Chem. Soc.* **2006**, 128, 6792.
- [18] C. de Mello Donegá, S. G. Hickey, S. F. Wuister, D. Vanmaekelbergh, A. Meijerink, *J. Phys. Chem. B* **2003**, 107, 489.

Supporting Information

© Wiley-VCH 2009

69451 Weinheim, Germany

Observation of a Ternary Nanocrystal Superlattice and Its Structural Characterization by Electron Tomography**

*Wiel H. Evers, Heiner Friedrich, Laura Fillion, Marjolein Dijkstra, and Daniel Vanmaekelbergh**

anie_200904821_sm_miscellaneous_information.pdf

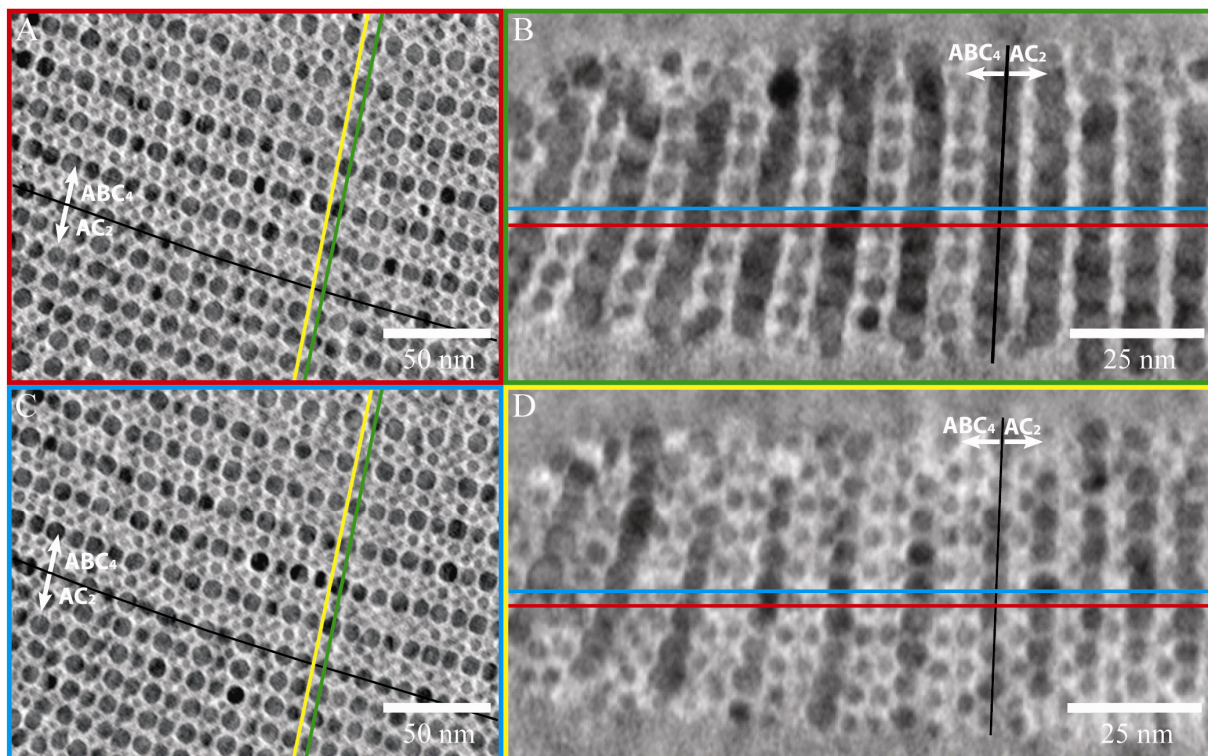


Figure S1: Reconstruction slices of the ternary superlattice ABC_4 (isostructural with $AlMgB_4$) epitaxially connected to a binary superlattice AC_2 (isostructural with AlB_2). A and C show horizontal cross sections separated by half a monolayer in height as is indicated in figures B and D. The green and yellow lines indicate the positions of the vertical cross sections displayed in B, D.

B and D present the epitaxy of the ternary structure (left hand side) to the binary AlB_2 structure. The cross section B cuts the large and medium sized PbSe NC; the cross section D cuts also the small CdSe NC.

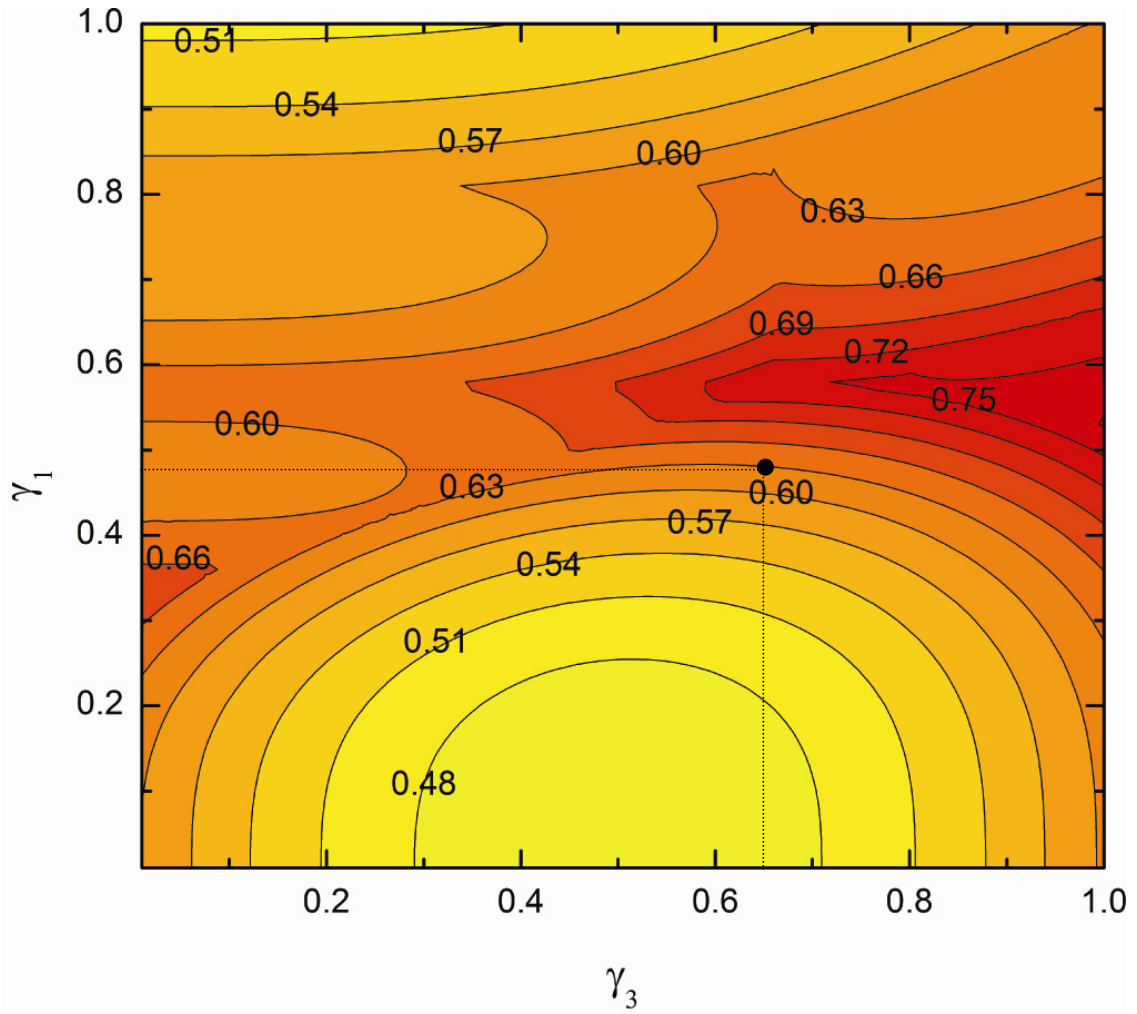


Figure S2: Contour plot of the maximum packing fraction of the ternary structure $AlMgB_4$ as a function of the size ratio's $\gamma_1 = \text{diameter small particle} / \text{large particle}$, and $\gamma_3 = \text{diameter medium sized particle} / \text{large particle}$. The maximum packing fraction was determined using Monte Carlo simulated annealing¹. Notice that there is a considerable region in which the maximum packing fraction of the ternary structure is similar tot that of a fcc single component lattice, indicating that the ternary structure $AlMgB_4$ might be stable. The point in which the $AlMgB_4$ structure was observed is indicated.

[1] L. Filion, M. Dijkstra, Phys. Rev. E, 79, 046714 (2009)